

Charge Transfer Processes in Conjugated Triarylamine–Oligothiophene–Perylenemonoimide Dendrimers

Andrea Petrella,[†] Jens Cremer,[‡] Luisa De Cola,[†] Peter Bäuerle,[‡] and René M. Williams^{*,†}

Molecular Photonic Materials, van 't Hoff Institute for Molecular Sciences, Universiteit van Amsterdam, Nieuwe Achtergracht 166, 1018 WS Amsterdam, The Netherlands, and Department Organic Chemistry II (Organic Materials and Combinatorial Chemistry), University of Ulm, Albert-Einstein-Allee 11, 89081 Ulm, Germany

Received: March 3, 2005; In Final Form: October 19, 2005

The synthesis and charge transfer properties of triarylamine–oligothiophene–perylene monoimide dendrimers, TPA(T₂-PMI)₃ and TPA(T₄-PMI)₃, are described. The fluorescence quantum yields indicate strong emission quenching by electron transfer [$\Phi_{\text{THF}} = 0.004$ for TPA(T₂-PMI)₃, $\Phi_{\text{THF}} = 0.003$ for TPA(T₄-PMI)₃, and $\Phi_{\text{THF}} = 0.8$ for PMI]. Moreover, with the increase of the solvent polarity, the quantum yields decrease indicating that the A⁺D⁻ (acceptor/donor) couple is more stabilized. The femtosecond transient absorption spectra show a very fast charge separation process (≈ 2 ps; $k_{\text{cs}} \approx 5 \times 10^{11} \text{ s}^{-1}$) and a charge recombination of more than 1 order of magnitude slower (≈ 50 ps; $k_{\text{cr}} \approx 2 \times 10^{10} \text{ s}^{-1}$), as observed from the rise time and decay of the radical anion and radical cation absorption bands. The analysis of the transient absorption spectroscopy and of the energetics of the process using Marcus theory indicates that in the electron transfer process the thiophene unit is the first electron donor. The triarylamine is not functioning as a second electron donor, as also substantiated by the absence of an effect of the addition of acid on the emission intensity of the dendrimers. The presence of the triarylamine and/or the proximity of the oligothiophenes does improve the donor capabilities of the oligothiophene unit slightly and enhances its conjugation as seen in the absorption spectra and the transients of the radical cations. These results can be used for a better design of molecular materials for, e.g., photovoltaic applications.

Introduction

Electron donor–acceptor systems^{1–3} are very attractive and promising candidates for applications in molecular and supramolecular electronics, light harvesting, and photocatalysis and also find important applications in organic photovoltaic cells,⁴ to convert sunlight into electrical energy.⁵ In recent years, there has been a great interest in preparing photoactive macromolecules on the nanometer scale, and among these, macromolecular dendrimers have drawn great interest due to their highly branched nature. This attention is not only from a synthetic point of view but also because they have very interesting and special physical and chemical properties.⁶ As dendrimers are also used as artificial photosynthetic systems, different types of dendritic chromophore assemblies have been designed in order to harvest light energy.^{7,8}

Recent synthetic developments enable the preparation of dendrimers with chromophores at the outer rims.^{9–12} By using this concept, a donor–acceptor dendrimer system, composed of peryleneimides at the edges with an oligophenyl spacer and a triphenylamine (TPA) as the core and as the donor, was reported. This system shows fast electron transfer and long-lived charge separation.¹³ In these systems, the photochemically stable peryleneimide acts as the electron acceptor in the excited state,¹⁴ while as the electron donor, TPA was chosen due to its importance as a hole transporter molecule in electrographic and

electroluminescent devices.^{15,16} In this context, there is not only a considerable interest in the study of photoinduced charge generation in covalently linked dyads but also in donor–donor–acceptor triads that include an additional moiety as a second electron donor.^{1–3,17}

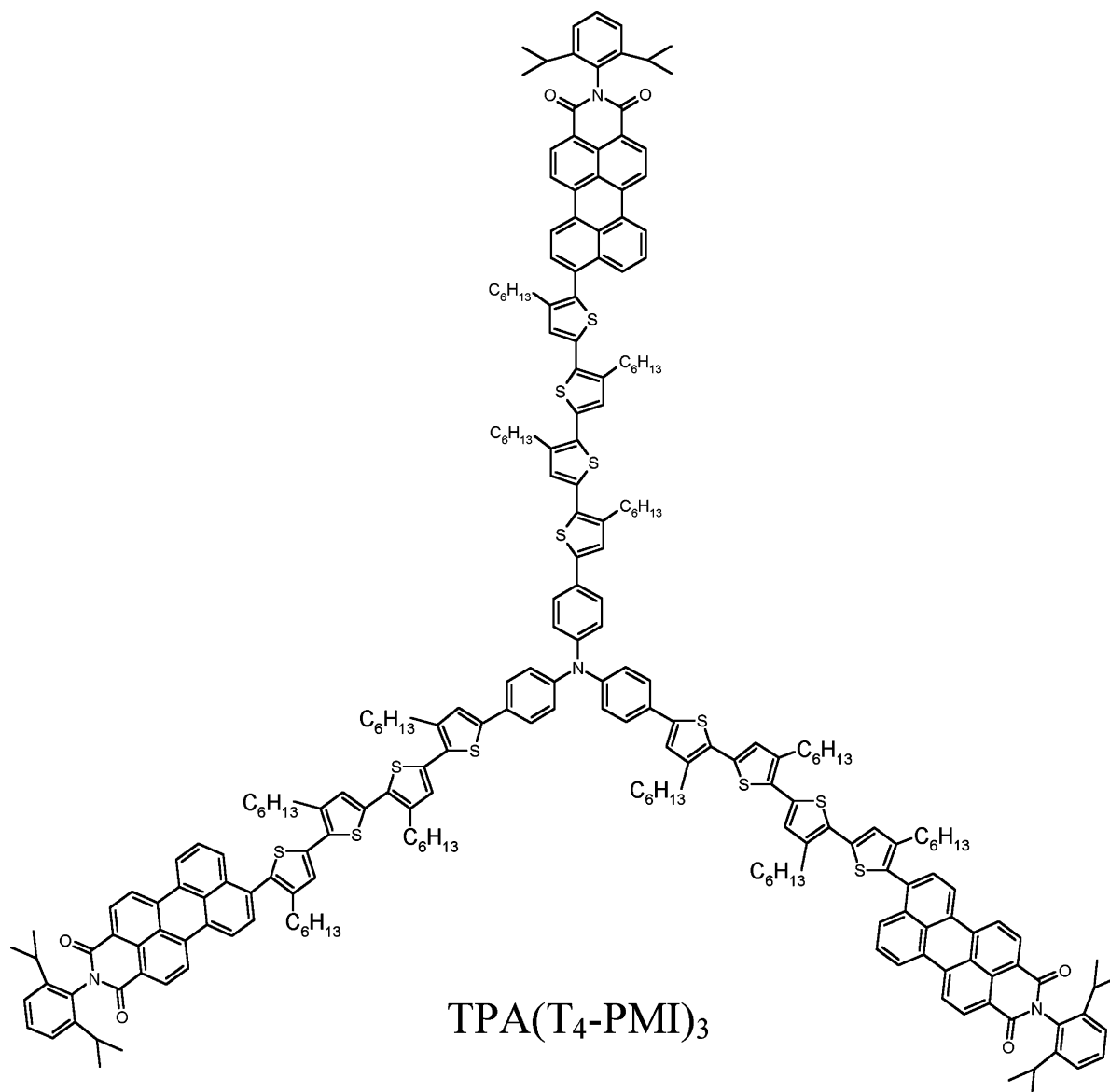
This paper presents the synthesis and the electron transfer processes in donor–donor–acceptor dendrimers with peryleneimide moieties at the periphery and an electron-donating TPA core substituted with oligothiophene units as the first electron donor. The role of oligothiophenes as a highly efficient energy and electron donor has been reported earlier.^{18–20} The investigated rigid peryleneimide dendrimers are the triarylamine–oligothiophene–perylene monoimide (PMI) dendrimers, TPA(T₂-PMI)₃ and TPA(T₄-PMI)₃, composed of the PMI as the acceptor and the oligothiophene and TPA moieties as the donors (see Schemes 1 and 3). Whereas structurally our system is similar to the one described by Lor et al.,¹³ our system contains an oligothiophene unit instead of an oligophenylene unit. The oligothiophene unit is expected to be a better conductor but is also much more easily oxidized.

To have a better understanding of the photophysics of the dendritic macromolecules, three reference systems have been analyzed as well (see Scheme 2). These molecules are PMI,²¹ sexithiophene (T₆),²² and perylene monoimide substituted with four thiophene units (PMI-T₄).²³ T₆ was chosen as a reference because it was readily available. Furthermore, the spectroscopy indicates that the four thiophene units are conjugated to the phenyl unit of the TPA unit and thus behave like a longer oligomer. Upon hindsight, TPA(T₂)₃ and TPA(T₄)₃ appear to be the ideal donor-reference molecules.

* To whom correspondence should be addressed. E-mail: williams@science.uva.nl.

[†] Universiteit van Amsterdam.

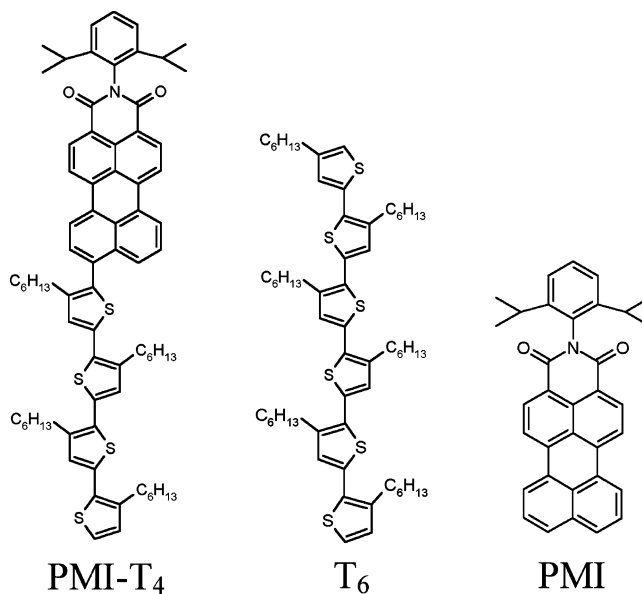
[‡] University of Ulm.

SCHEME 1: Molecular Structure of the Triarylamine–Oliothiophene–PMI Dendrimer TPA(T₄-PMI)₃**Results and Discussion**

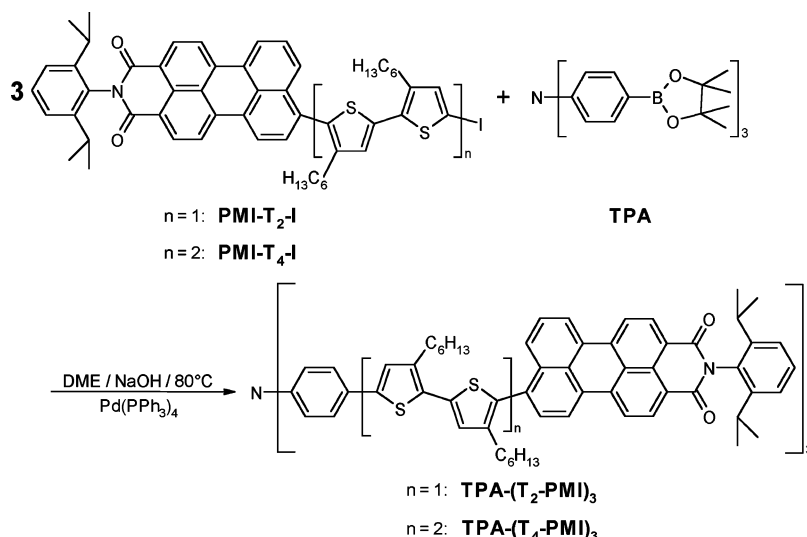
Synthesis. The dendrimer TPA(T₂-PMI)₃ was synthesized in 62% yield via palladium(0)-catalyzed coupling of iodinated perylenyl-oligothiophene PMI-T₂-I²³ and the 3-fold boronic ester of TPA in DME at 80 °C. The longer homologue, TPA(T₄-PMI)₃, was similarly obtained in 54% yield by reacting TPA boronic ester with PMI-T₄-I under the same reaction conditions (see Scheme 3).²⁴

Steady-State Spectroscopy. The UV–vis absorption and luminescence spectra of TPA(T₂-PMI)₃, TPA(T₄-PMI)₃, PMI-T₄, T₆, and PMI in tetrahydrofuran (THF) are depicted in Figures 1 and 2, respectively. The absorption maxima that correspond to, respectively, the oligothiophene unit and the peryleneimide are observed at 402 and 513 [for TPA(T₂-PMI)₃], 428 and 513 [for TPA(T₄-PMI)₃], and 364 and 515 nm (for PMI-T₄). For the reference systems, these absorptions are observed at 478 and 501 (for PMI) and 403 nm (for T₆).

Figure 1a shows that in the 400–600 nm range the absorption bands of TPA(T₂-PMI)₃ and TPA(T₄-PMI)₃ are substantially broadened as compared to the PMI itself. Furthermore, the absorption bands of the oligothiophene units within the dendrimers can be identified at 402 and 428 nm. The broadening

SCHEME 2: Molecular Structure of the Three Reference Compounds

SCHEME 3: Synthetic Scheme for the Two Dendrimers



effect of the PMI based absorption can be attributed to the more delocalized electron distribution in the dendrimers, also pointed out by the red shifted and broadened emission bands of the dendrimers, as compared to PMI (Figures 2 and 3). The broadening of the absorption bands may also be attributed to a small amount of charge transfer character in the ground state. It can also be noticed that the difference in absorption maxima of the oligothiophene band of PMI- T_4 ($\lambda_{\max} = 364$ nm) and TPA(T_4 -PMI) $_3$ ($\lambda_{\max} = 428$ nm) clearly shows the effect of the

conjugation of the (phenyl unit of) TPA with the oligothiophene unit. Figure 2 shows clearly that, relative to the components PMI and T₆, the emission of the dendrimers (and of PMI- T_4) is fully quenched. The emission spectra of the two dendrimers are also presented separately in Figure 3. The emission maxima are given in Table 1.

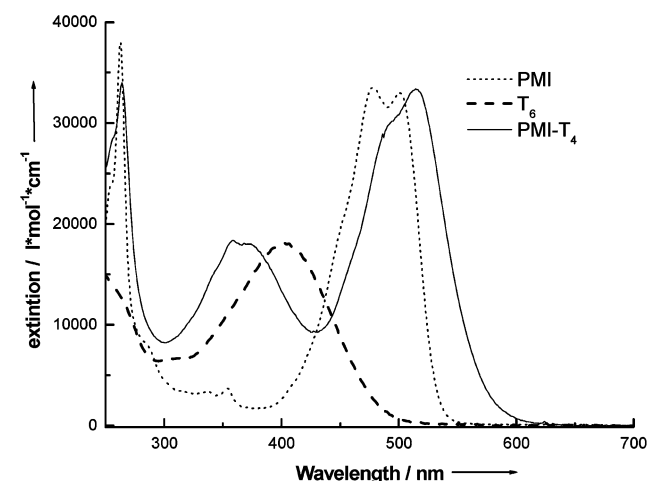
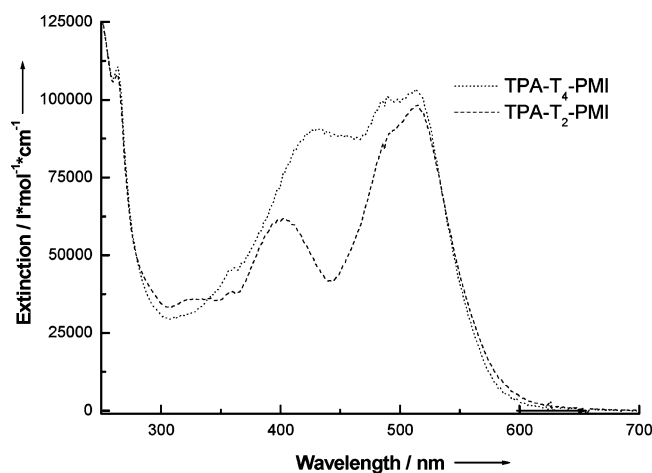


Figure 1. Absorption spectra of (a) TPA(T_2 -PMI) $_3$ and TPA(T_4 -PMI) $_3$ in THF and (b) PMI, PMI- T_4 , and T₆ in THF.

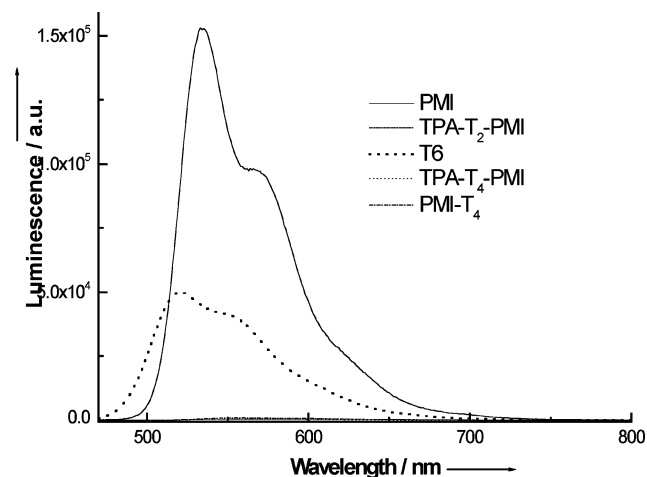


Figure 2. Luminescence spectra of TPA(T_2 -PMI) $_3$, TPA(T_4 -PMI) $_3$, PMI (strongest signal), PMI- T_4 , and T₆ in THF ($\lambda_{\text{ex}} = 460$ nm).

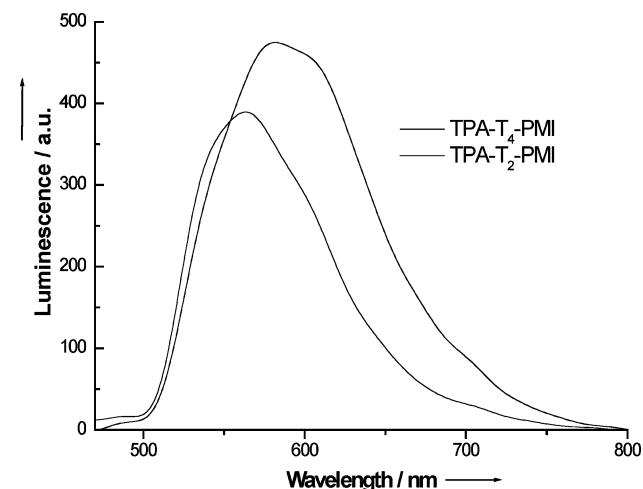


Figure 3. Magnification of luminescence spectra of TPA(T_2 -PMI) $_3$ (strongest signal), and TPA(T_4 -PMI) $_3$ in THF reported in Figure 2.

TABLE 1: Emission Maxima (λ_{em}) and Fluorescence Quantum Yields (Φ) of TPA(T₂-PMI)₃, TPA(T₄-PMI)₃, PMI-T₄, PMI, and T₆ in THF, CHCl₃, and Toluene^a

	THF ($\epsilon = 7.58$)		chloroform ($\epsilon = 4.70$)		toluene ($\epsilon = 2.38$)	
	λ_{em} (nm)	Φ	λ_{em} (nm)	Φ	λ_{em} (nm)	Φ
TPA(T ₂ -PMI) ₃	582	0.004	590	0.007	634	0.03
TPA(T ₄ -PMI) ₃	562	0.003	574	0.003	644	0.03
PMI-T ₄	555	0.012	565	0.014	627	0.04
PMI	535	0.80	539	0.80	532	0.80
T ₆	520	0.28	526	0.33	523	0.45

^a $\lambda_{ex} = 460$ nm. Emission standard: N,N'-bis-(2,5-di-*tert*-butylphenyl)-3,4,9,10-perylene-tetracarboxylic acid diimid ($\Phi = 0.99$ in CHCl₃).

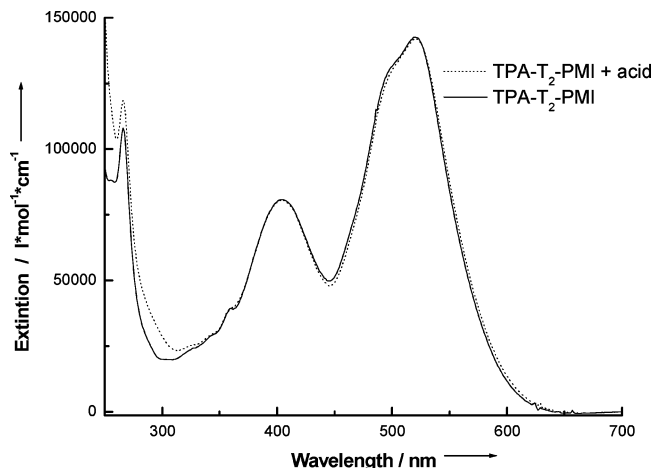
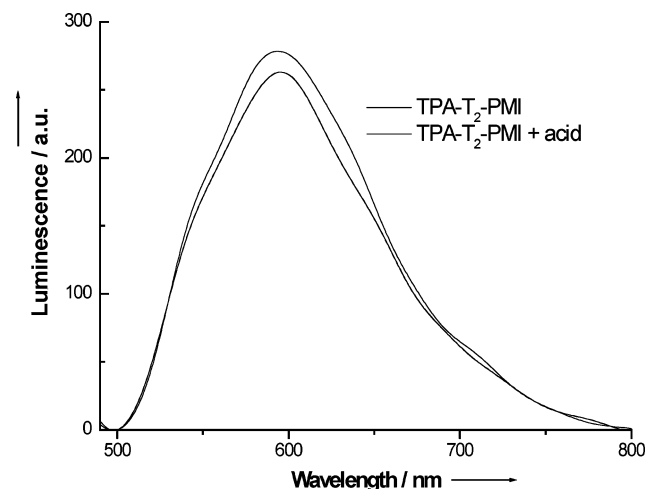
To have a more complete analysis of the investigated systems, steady-state spectroscopy was also conducted in chloroform and toluene solutions. Table 1 summarizes the wavelengths of the emission maxima of the dendrimers and reference compounds. Interestingly, the dendritic emission shows a hypsochromic shift with increasing solvent polarity. No solvent effect was observed in the absorption spectra of the samples. This blue shift of the emission of TPA(T₂-PMI)₃ and TPA(T₄-PMI)₃ (also observed for PMI-T₄) with solvent polarity increase is surprising. Normally, the local emission of the acceptor or donor does not shift significantly with polarity.²⁵ The charge transfer emission normally shifts to the red upon increasing solvent polarity.²⁶ Similar hypsochromic shifts were observed before for related systems but were not discussed.¹³

The hypsochromic shift effect is tentatively explained by a mixing of local perylene excited state with the charge transfer state and a change of the effective center-to-center distance²⁷ that becomes smaller in nonpolar solvents due to Coulombic effects. The oligomeric nature of the donor will allow a solvent-dependent radical cation center by which the center-to-center distance between the donor and the acceptor can be modulated. In polar solvents, solvation effects will prevail, and the most effective stabilization where both ions are solvated separately by oriented solvent shells will occur at an increased effective distance.

In Table 1, the fluorescence quantum yields of the systems are also reported.²⁸ As an emission standard for the PMI systems, N,N'-bis-(2,5-di-*tert*-butylphenyl)-3,4,9,10-perylene-tetracarboxylic acid bisimide ($\Phi = 0.99$ in CHCl₃) was used.²⁹ The quantum yields of the emission of the dendrimers (and for PMI-T₄) are very low with respect to the values obtained for PMI and T₆, which suggests electron transfer quenching in TPA(T₂-PMI)₃ and TPA(T₄-PMI)₃ (and in PMI-T₄). By using $k_{et} = (\Phi_0/\Phi - 1)/\tau_0$, we can give an (lower) estimate of the rate of TPA(T₄-PMI)₃ in THF of $5.6 \times 10^{10} \text{ s}^{-1}$.

For PMI-T₄, it is observed that the maximum of emission is more blue-shifted as compared to the dendritic molecules and that the quantum yields are slightly higher with respect to the values obtained for TPA(T₄-PMI)₃ (Table 1). The blue shift of emission is attributed to a less extensive electron delocalization in PMI-T₄, which moreover is in agreement with the less broad absorption band (Figure 1). The emission quantum yields of PMI-T₄ are very low with respect to those obtained for PMI, indicating electron transfer quenching by the thiophene (donor), but are higher than those of the TPA(T₄-PMI)₃. This indicates that in TPA(T₄-PMI)₃, the conjugation with (the phenyl unit of) TPA and/or the proximity of the three oligothiophene units makes T₄ a better donor. The quantum yields of PMI and T₆ agree well with the values reported in the literature.^{30,31}

Table 1 shows that the emission quantum yields of TPA(T₂-PMI)₃ and TPA(T₄-PMI)₃ and PMI-T₄ decrease with

**Figure 4.** Absorption spectra of TPA(T₂-PMI)₃ in CHCl₃ before and after the addition of few microliters of trifluoroacetic acid.**Figure 5.** Luminescence spectra of TPA(T₂-PMI)₃ in CHCl₃ before and after (strongest signal), the addition of few microliters of trifluoroacetic acid ($\lambda_{ex} = 460$ nm).

increasing polarity, which indicates that the charge transfer state ($A^{\bullet-}D^{\bullet+}$) is stabilized more with the increasing of the solvent polarity, which moreover influences the TPA(T₄-PMI)₃ system slightly more than TPA(T₂-PMI)₃ and PMI-T₄.

As the charge transfer state is located at ca. 1.5 eV (826 nm) above the ground state in THF (see Energetics) and at ca. 1.9 eV (650 nm) in chloroform and no emission is observed at these wavelengths, no radiative decay of the charge transfer state occurs. In toluene as a solvent, the situation is not fully clear (as charge separation is expected to be endergonic) due to the oligomeric nature of the oligothiophene donor that appears to modulate the center-to-center distance depending on the solvent. Further studies are needed here.

The effects of the addition of acid on the absorptive and emissive properties of TPA(T₂-PMI)₃ were studied in CHCl₃. After the addition of a few microliters of trifluoroacetic acid, negligible changes in the spectra were observed (see Figures 4 and 5). Clearly, protonation of the TPA nitrogen, which nullifies the electron-donating properties²⁵ of TPA, indicates that in the donor-donor-acceptor triad the thiophene unit is the first and only electron donor and the TPA unit does not play a role as a second electron donor (*vide infra*).

The emission spectra were recorded upon 460 nm excitation. The ratio of the absorption at 460 nm of the T₄ unit and the PMI unit in, e.g., TPA(T₄-PMI)₃, is estimated from Figure 1 to be 1:1. Because of the strong conjugation of the two chro-

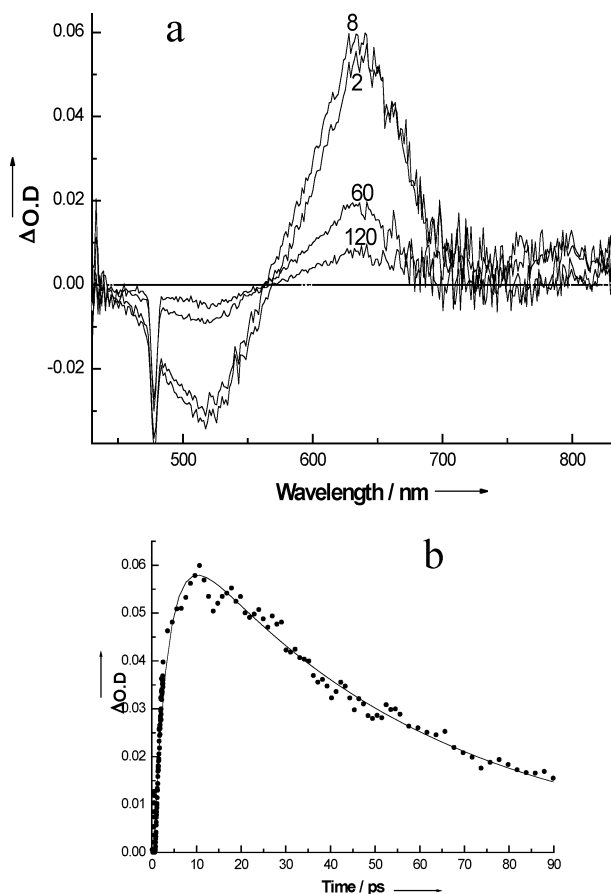


Figure 6. (a) Transient absorption spectra of TPA(T₂-PMI)₃ in THF at 2, 8, 60, and 120 ps of time delay ($\lambda_{\text{ex}} = 480$ nm). (b) Rise time and decay of the ion-pair absorption at $\lambda_{\text{detec}} = 639$ nm.

TABLE 2: Charge Separation Time τ_{rise} and Charge Transfer State Lifetime τ_{decay} of TPA(T₂-PMI)₃, TPA(T₄-PMI)₃, and PMI-T₄ Measured in THF by Means of Femtosecond Transient Absorption Spectroscopy ($\lambda_{\text{ex}} = 480$ nm) Together with the Corresponding Rates

	τ_{rise} (ps) [A ₁]	τ_{decay} (ps) [A ₁]	κ_{rise} (s ⁻¹)	κ_{decay} (s ⁻¹)
TPA(T ₂ -PMI) ₃	2.8 [-0.018]	46 [0.031]	3.6×10^{11}	2.2×10^{10}
TPA(T ₄ -PMI) ₃	1.6 [-0.020]	66 [0.024]	6.2×10^{11}	1.5×10^{10}
PMI-T ₄	4.6 [-0.380]	49 [0.580]	2.2×10^{11}	2.0×10^{10}

mophores, it is not possible to give exact numbers. For the “separate” nonbonded chromophores, selective excitation would occur. The charge transfer processes in TPA(T₂-PMI)₃ and TPA(T₄-PMI)₃ and in PMI-T₄ were investigated by further study with time-resolved spectroscopy.

Time-Resolved Spectroscopy. Single photon counting and nanosecond transient absorption in THF as a solvent indicate that the charge separation and charge recombination occur on a very fast time scale, faster than the time limits of these techniques. The emissive lifetimes of PMI and T₆, in THF, were determined to be, respectively, 4.74 and 0.76 ns.

Femtosecond Transient Absorption Spectroscopy. By means of femtosecond transient absorption spectroscopy ($\lambda_{\text{ex}} = 480$ nm), the rise times and decay times of the radical anion and cation absorption were determined. The spectra of TPA(T₂-PMI)₃, TPA(T₄-PMI)₃, and PMI-T₄ are shown in Figures 6–8, respectively; the rise and decay times obtained from the femtosecond transient absorption data are summarized in Table 2.

As can be seen in Figure 7, also a very fast component (≈ 0.3 ps) is present on the red side of the spectrum of TPA(T₄-PMI)₃

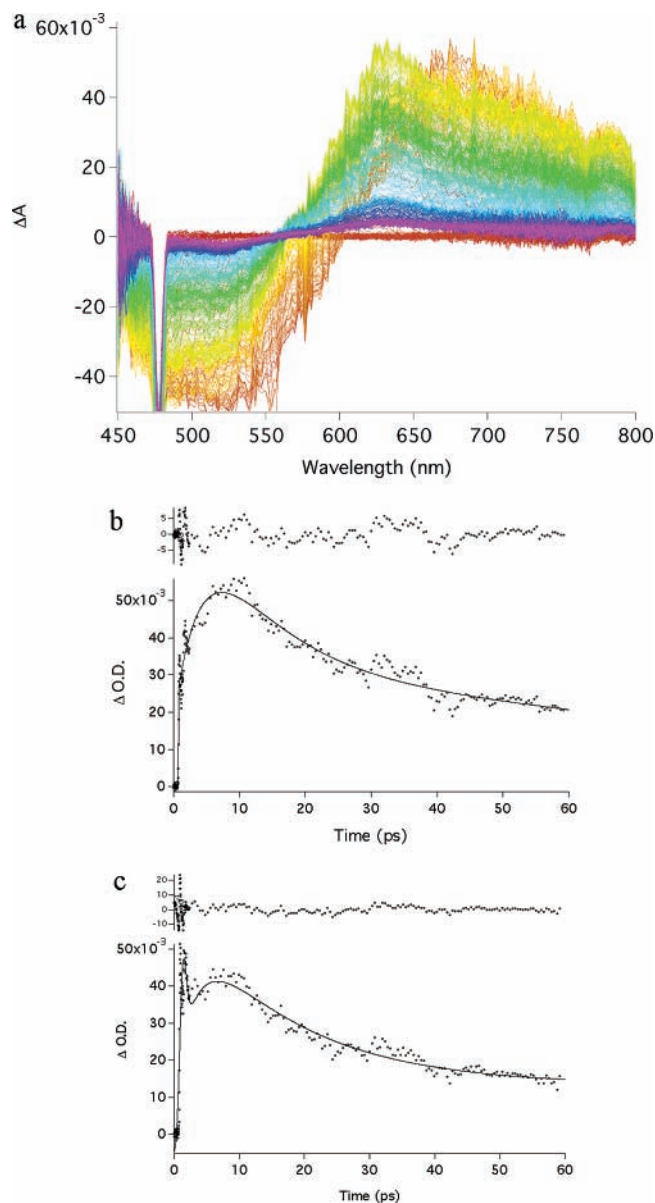


Figure 7. (a) Femtosecond transient absorption spectra of TPA(T₄-PMI)₃ in THF at all incremental time delays recorded ($\lambda_{\text{ex}} = 480$ nm). (b) Rise time and decay of the ion-pair absorption at $\lambda_{\text{detec}} = 640$ nm. (c) Ultrafast component and rise time and decay of the ion-pair absorption at $\lambda_{\text{detec}} = 680$ nm.

that can be attributed to energy transfer from the oligothiophene unit to the PMI moiety and solvation processes (see the Supporting Information for the T₆ spectrum). The fast decaying 680 nm band is attributed to the singlet–singlet absorption of the oligothiophene unit.

Comparison of the spectra in the 600–800 nm region shows an interesting spectral difference with a striking structured feature at 790 nm for PMI-T₄ (Figure 8) and TPA(T₄-PMI)₃ (Figure 7). Fortunately, the radical cation spectra of oligothiophenes of different lengths have received ample attention^{32,33} and show a systematic red shift upon increase of conjugation length. Furthermore, similar spectral features, as observed here at 790 nm, are observed for the radical cations of pentameric oligothiophenes, and terthiophenes show absorption bands around 620 nm. So clearly, the radical cation and anion absorption of TPA(T₂-PMI)₃ coincide (Figure 6). For PMI-T₄, the structured feature at 790 nm can be attributed to the radical cation of T₄ (Figure 8), and for TPA(T₄-PMI)₃, the spectral gap,

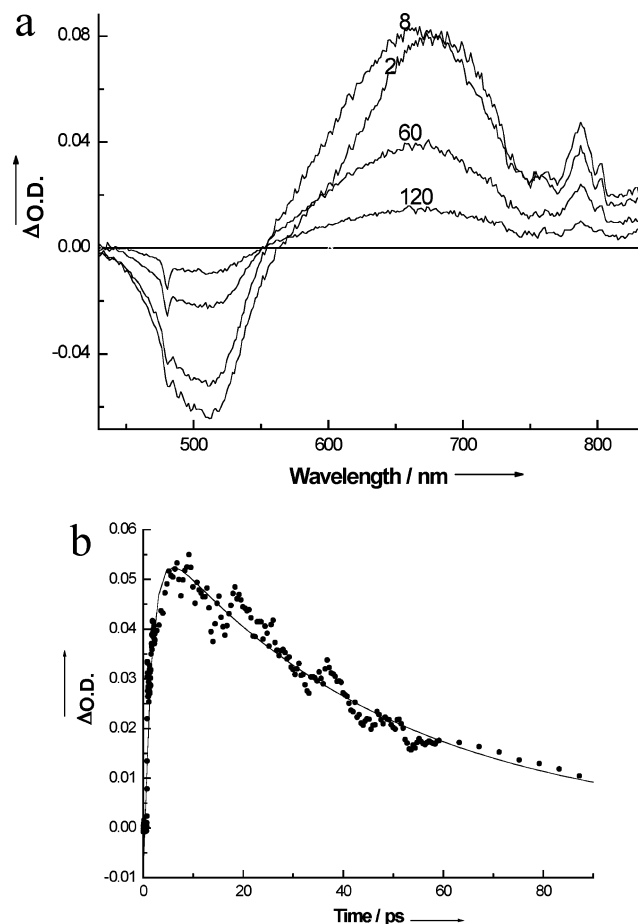


Figure 8. (a) Femtosecond transient absorption spectrum of PMI-T₄ in THF at 2, 8, 60, and 120 ps of time delay ($\lambda_{\text{ex}} = 480$ nm). (b) Rise and decay of the ion-pair absorption of PMI-T₄ at $\lambda_{\text{detec}} = 611$ nm.

between the radical anion absorption at 630 nm and the radical cation feature at 790 nm, is filled due to the enhanced conjugation of the oligothiophene to the (phenyl unit of) TPA unit. The radical cation absorption bands observed here are slightly red-shifted with respect to the values reported in the literature.^{32,33} This effect can be explained by the high delocalization in the molecules due to conjugation with (the PMI and) the phenyl unit of the TPA, which shifts the absorption to slightly lower energies and which furthermore enhances band broadening. In all femtosecond transient absorption spectra, the radical anion absorption of the peryleneimide (at 630–640 nm)¹³ is observed and is formed with a 2–5 ps rise time (see Table 2). The radical cation absorption bands around 790 nm for PMI-T₄ and TPA(T₄-PMI)₃ show a similar rise time. Because we do not have selective excitation of the perylene chromophore, also due to the strong coupling between the chromophoric units, energy transfer to the perylene and some short-lived singlet–singlet absorption of the perylene is also present.³⁴ All dark states decay by vibrational relaxation. The rates of the electron transfer processes are in the order of a few picoseconds. The energy transfer is 1 order of magnitude faster. The rate of charge recombination is more than 1 order of magnitude slower (charge transfer state lifetime $\tau \approx 50$ ps).

Figure 9 shows a comparison of the spectra (at 8 ps time delay) of the three systems. The 790 nm band is clearly present in TPA(T₄-PMI)₃ and in PMI-T₄. The radical cation absorption band is due to the T₄ unit and is only slightly perturbed by its substitution in TPA(T₄-PMI)₃. Figure 9 also points out that the transient absorption of PMI-T₄ is very similar to that of the

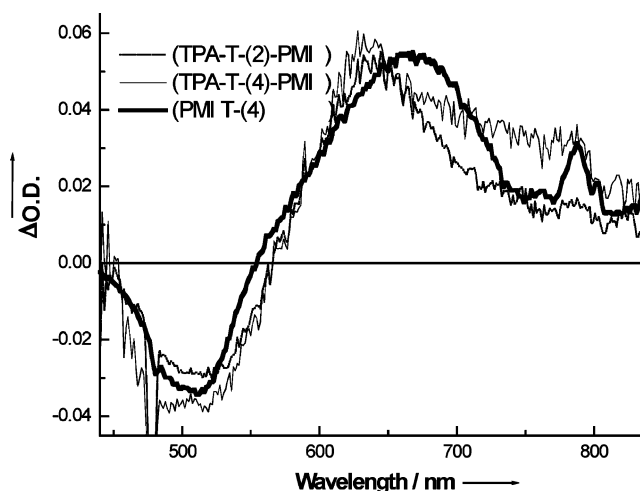


Figure 9. Comparison of the femtosecond transient absorption spectra of TPA(T₂-PMI)₃, TPA(T₄-PMI)₃, and PMI-T₄ in THF at 8 ps time delay ($\lambda_{\text{ex}} = 480$ nm).

TPA(T₄-PMI)₃ and TPA(T₂-PMI)₃ dendrimers. Moreover, from the analysis of the peryleneimide radical anion lifetime in PMI-T₄, it can be observed that the forward electron transfer and the charge recombination process occur almost on the same time scale as for TPA(T₄-PMI)₃ and TPA(T₂-PMI)₃. In other words, the absence of the TPA unit in the reference system does not change the kinetics of the charge transfer processes. This also implies that singlet–singlet or singlet–CT annihilation in the multichromophoric dendrimers does not occur on a significant scale.

The radical cation spectrum of TPA is well-established³⁵ and shows maxima at 358, 562, and 650 nm for TPA itself, while this is already perturbed by the presence of an extra phenyl group³⁶ to 397, 695, and 772 nm. On the basis of the spectral features observed in the femtosecond transient absorption spectroscopy and the absence of an effect of acid addition on the steady-state emission, we conclude that the TPA unit is not oxidized by the acceptor upon photoexcitation. The results obtained with the time-resolved spectroscopy suggest that in the two dendrimers the thiophene unit is the first and only electron donor (Table 2).

The femtosecond transient absorption of PMI and of T₆ (see Supporting Information) resulted in long-lived species with the following maxima and lifetimes: For PMI, a strong transient absorption band is observed at 620 nm with a lifetime longer than 3 ns (the emission lifetime determined with SPC is 4.7 ns). This is attributed to S₁ to S_n absorption [$\tau_{(620\text{nm})}$ (S₁) > 3 ns]. For T₆, an initial transient absorption band at 800 nm is observed, which transforms with a 350 ps time constant to an absorption band at 700 nm that has a long lifetime and is attributed to the triplet state [$\tau_{(800\text{nm})}$ (S₁) \approx 350 ps; $\tau_{(700\text{nm})}$ (T₁) > 2 ns]. Fast processes related to solvent relaxation for PMI are observed, as also reported for perylenebisimide systems^{34,37} but in general have only a minor amplitude. The large difference between the spectral and the kinetic behavior of PMI-T₄, TPA(T₄-PMI)₃, and TPA(T₂-PMI)₃ relative to PMI and T₆, together with the strong quenching of the emission, clearly shows the special behavior of the active systems.

The transient absorption spectra were recorded upon 480 nm excitation. The ratio of the absorption at 480 nm of the T₄ unit and the PMI unit in, e.g., TPA(T₄-PMI)₃, is estimated from Figure 1 to be 1:10. Because of the strong conjugation of the two chromophores, it is not possible to give exact numbers.

TABLE 3: Calculated Values of Standard Gibbs Free Energy Change ΔG_{cs} (Driving Force), Barrier to Charge Separation (ΔG^*), and λ (Reorganization Energy) for TPA(T_2 -PMI) $_3$ and TPA(T_4 -PMI) $_3$ for the Electron Transfer Processes TPA \rightarrow PMI and (Oligothiophene) $T_n \rightarrow$ PMI^a

	THF ($\epsilon = 7.58$)			chloroform ($\epsilon = 4.70$)			toluene ($\epsilon = 2.38$)		
	ΔG_{cs} (eV)	λ (eV)	ΔG^* (eV)	ΔG_{cs} (eV)	λ (eV)	ΔG^* (eV)	ΔG_{cs} (eV)	λ (eV)	ΔG^* (eV)
TPA \rightarrow PMI									
TPA(T_2 -PMI) $_3$	-0.46	1.51	0.18	-0.07	1.16	0.26	0.74	0.38	0.82
TPA(T_4 -PMI) $_3$	-0.48	1.56	0.19	-0.15	1.22	0.23	0.72	0.39	0.79
$T_n \rightarrow$ PMI									
TPA(T_2 -PMI) $_3$	-0.76	1.30	0.06	-0.46	1.01	0.08	0.21	0.37	0.22
TPA(T_4 -PMI) $_3$	-0.69	1.45	0.10	-0.39	1.12	0.12	0.40	0.38	0.40

^a The internal reorganization energy λ_i is 0.3 eV. In TPA(T_2 -PMI) $_3$, the TPA \rightarrow PMI distance is $R_c = 17$ Å while the $T_n \rightarrow$ PMI distance is $R_c = 10$ Å; in TPA(T_4 -PMI) $_3$, the TPA \rightarrow PMI distance is $R_c = 23$ Å while the $T_n \rightarrow$ PMI distance is $R_c = 14$ Å. An E_{00} of 2.3 eV was used.

TABLE 4: Electrochemistry of TPA(T_2 -PMI) $_3$ and TPA(T_4 -PMI) $_3$, TPA, and PMI^a

	$E^0\text{Red}_2$ (V)	$E^0\text{Red}_1$ (V)	$E^0\text{Ox}_1$ (V)	$E^0\text{Ox}_2$ (V)	$E^0\text{Ox}_3$ (V)	$E^0\text{Ox}_4$ (V)	$E^0\text{Ox}_5$ (V)
TPA				+0.53			
TPA(T_2 -PMI) $_3$	-1.86	-1.39	+0.28	+0.56	+0.76	+0.95	+1.16
TPA(T_4 -PMI) $_3$	-1.87	-1.40	+0.27	+0.42	+0.66	+1.03	+1.13
PMI	-1.95 ^b	-1.46 ^b					

^a Measurements conducted in dichloromethane, 10 mV/s, 0.1 M TBAHFP vs ferrocene/ferrocenium. ^b Taken from ref 21.

For the “separate” nonbonded chromophores, selective excitation would occur.

Energetics. To have a more complete view of the forward charge transfer process, the analysis of the driving forces and the energy barriers in the different solvents was performed. The effect of the solvent polarity on the charge separation processes is related to the stabilization of the product state with respect to the initial state. For photoinduced charge separation, this is conveniently quantified by the so-called Weller type analysis³⁸:

$$\Delta G = e[E_{\text{OX}}(\text{D}) - E_{\text{red}}(\text{A})] - E_{00} - \frac{e^2}{4\pi\epsilon_0\epsilon_S R_C} - \frac{e^2}{8\pi\epsilon_0} \left(\frac{1}{r^+} + \frac{1}{r^-} \right) \left(\frac{1}{\epsilon_{\text{CH}_2\text{Cl}_2}} - \frac{1}{\epsilon_S} \right) \quad (1)$$

which relates the standard Gibbs energy change (driving force) in a medium with static dielectric constant ϵ_S to the standard redox potentials of the donor (D) and the acceptor (A) (as measured in dichloromethane, i.e., at $\epsilon_S = 8.93$), the E_{00} excitation energy of either D or A, their center to center separation R_C , and the average ionic radius of D^+ and A^- .

The R_C distances were determined by molecular modeling, assuming that the charges are located at the centers of the donor and acceptor units. In this case, a comparison of the driving forces in the three solvents of different polarity (THF, CHCl_3 , and toluene) was made for two different charge transfer processes in TPA(T_2 -PMI) $_3$ and in TPA(T_4 -PMI) $_3$ molecules: TPA(donor) \rightarrow PMI (acceptor) or thiophene(donor) \rightarrow PMI-(acceptor) (Table 3) (in these calculations, $r^+ = 4$ Å, $r^- = 3$ Å, and the electrochemistry has been conducted in dichloromethane, 0.1 M TBAHFP vs ferrocene/ferrocenium as shown in Table 4).

A representative cyclic voltammogram is given in Figure 10. In the case of the charge transfer between PMI and TPA in

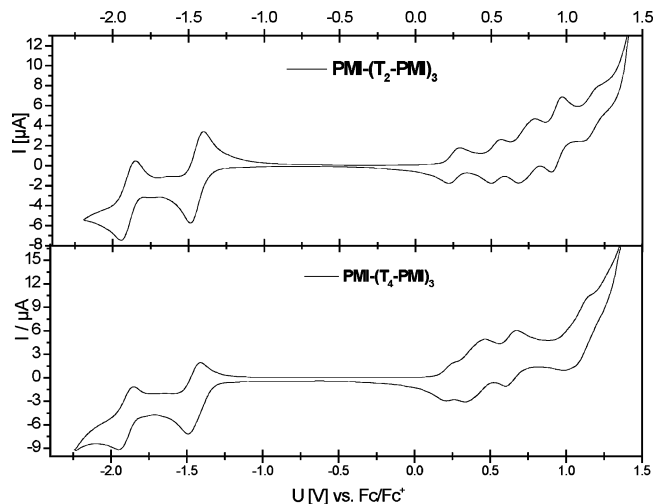


Figure 10. Cyclic voltammograms of TPA(T_2 -PMI) $_3$ and TPA(T_4 -PMI) $_3$ in dichloromethane/TBAHFP (0.1 M) vs Fc/Fc⁺ at 100 mV/s.

TPA(T_4 -PMI) $_3$ and TPA(T_2 -PMI) $_3$, the oxidation potentials are +0.42 and +0.56 V (vs ferrocene/ferrocenium), respectively, corresponding to the TPA oxidation,³⁹ while in the case of the charge transfer between PMI and thiophene in TPA(T_4 -PMI) $_3$ and TPA(T_2 -PMI) $_3$, the oxidation potentials are +0.27 and +0.28 V (vs ferrocene/ferrocenium), respectively, corresponding to the thiophene oxidation.⁴⁰ The reduction potentials of the two dendrimers are due to the reduction of the peryleneimide unit [-1.40 V for TPA(T_4 -PMI) $_3$ and -1.39 V for TPA(T_2 -PMI) $_3$ (vs ferrocene/ferrocenium)].²¹

Furthermore, values for the barrier to charge separation (ΔG^*) can be estimated via the classical Marcus equation:⁴¹

$$\Delta G^* = \frac{(\Delta G + \lambda)^2}{4\lambda} \quad (2)$$

where $\lambda = \lambda_I + \lambda_S$.

λ_S is the solvent reorganization term, while λ_I (0.3 eV) is the internal reorganization energy.

$$\lambda_S = \frac{e^2}{4\pi\epsilon_0} (1/r - 1/R_C) (1/n^2 - 1/\epsilon_S) \quad (3)$$

where r is the average ionic radius and n is the solvent refractive index (Table 3).

The values of ΔG , λ , and ΔG^* calculated on the basis of the eqs 1–3 show that the charge transfer is in the Marcus normal region ($-\Delta G < \lambda$), and as the solvent polarity increases, the $A^- D^+$ charge-separated state is stabilized. These effects result in the reduction of the energy barrier for the charge transfer between donor and acceptor in the more polar solvents. Furthermore, the more energetically favorable processes are charge transfer between thiophene and PMI in both of the dendrimers, with a lower energy barrier for the charge transfer in TPA(T_2 -PMI) $_3$ (0.06 eV in THF) with respect to TPA(T_4 -PMI) $_3$ (0.10 eV in THF). It is interesting to notice that in toluene emission quenching is observed, although the driving force is absent according to the data in Table 3. Either the quadrupole moment of toluene is responsible or a shorter effective center-to-center distance should be applied (which would again be due to the oligomeric nature of the thiophene donor). The photo-physical properties in THF, together with the energetics, are summarized in Figure 11.

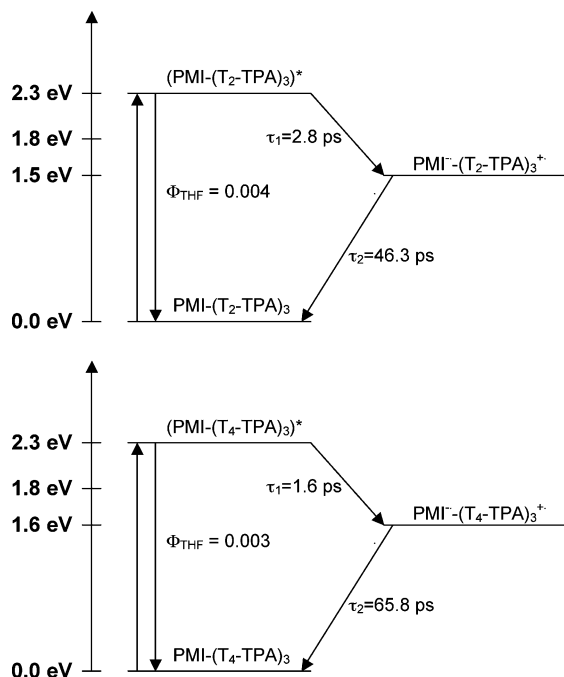


Figure 11. Energetic schemes of $\text{TPA}(\text{T}_2\text{-PMI})_3$ and $\text{TPA}(\text{T}_4\text{-PMI})_3$ in THF, indicating the specific times for charge separation and charge recombination, as well as the quantum yield of emission.

Conclusions

The synthesis and charge transfer properties of triarylamine–oligothiophene–PMI dendrimers, $\text{TPA}(\text{T}_2\text{-PMI})_3$ and $\text{TPA}(\text{T}_4\text{-PMI})_3$, were established. Fast photoinduced electron transfer ($\tau \approx 2$ ps) and strongly quenched emission [$\Phi_{\text{THF}} = 0.004$ for $\text{TPA}(\text{T}_2\text{-PMI})_3$ and $\Phi_{\text{THF}} = 0.003$ for $\text{TPA}(\text{T}_4\text{-PMI})_3$] were observed. Moreover, the quantum yields of emission decrease with increasing polarity indicating that the $\text{A}^{+\bullet}\text{D}^{-\bullet}$ (acceptor/donor) couple is more stabilized with the increase of the solvent polarity.

Calculation of the energy barriers to the electron transfer yields to a reduction of the ΔG^* for the charge transfer between donor and acceptor in the more polar solvents resulting in an increase of the rates for the charge separation. Furthermore, the more energetically favorable processes are the charge transfer processes between oligothiophene unit and PMI in both of the dendrimers.

Besides energetic analysis, the steady-state emission spectra obtained upon acid addition and femtosecond transient absorption spectra show that in the electron transfer process the thiophene unit is the first and only electron donor. The triarylamine is not functioning as a second electron donor, but it does improve the donor capabilities of the oligothiophene unit and enhances its conjugation as seen in the absorption spectra, the transients of the radical cations, and the quantum yields of emission. Because the oligothiophene donor and the PMI acceptor are linked by one single bond, through space interaction is considered not important. Very recently, a bithiophene–PMI system was studied⁴² that displays a slower charge separation as observed here. It is interesting to notice also that the steady-state emission quenching is much more pronounced in $\text{TPA}(\text{T}_2\text{-PMI})_3$ than in PMI-T_2 , again indicating that the donor properties of the oligothiophene are improved by TPA substitution and that charge transfer is the main process in $\text{TPA}(\text{T}_2\text{-PMI})_3$. Furthermore, an increase of the oligothiophene length results in a steady increase of donor strength as well as a steady red shift of the radical cation absorption. TPA substitution has

a similar effect. Thus, triarylamine substitution of oligothiophenes can improve the thiophene donor capabilities and result in faster charge separation. These results can be used for a better design of molecular materials for, e.g., photovoltaic applications.

Experimental Section

Photophysical Properties. Electronic absorption spectra were recorded on a Hewlett-Packard UV–vis, diode array 8453 spectrophotometer. Steady-state emission spectra were obtained from SPEX 1681 Fluorolog spectrofluorimeter equipped with two double monochromator (excitation and emission) and are corrected for the photomultiplier response. Quantum yields of compounds were measured with respect to *N,N'*-bis-(2,5-di-*tert*-butylphenyl)-3,4,9,10-perylene-tetracarboxylic acid bisimide ($\Phi = 0.99$ in CHCl_3) purchased from Aldrich. Both solvents used were spectroscopic grade and purchased from Acros and Merck Uvasol. Trifluoroacetic acid was purchased from Janssen Chimica.

Time-resolved fluorescence measurements were performed on a picosecond single photon counting (SPC) setup. The frequency-doubled (300–340 nm, 1 ps, 3.8 MHz) output of a cavity dumped DCM dye laser (Coherent model 700) pumped by a mode-locked Ar-ion laser (Coherent 486 AS Mode Locker, Coherent Innova 200 laser) was used as the excitation source. A (Hamamatsu R3809) microchannel plate photomultiplier was used as detector. The instrument response (~ 17 ps fwhm) was recorded using the Raman scattering of a doubly deionized water sample. Time windows (4000 channels) of 5 (1.25 ps/channel) to 50 ns (12.5 ps/channel) could be used, enabling the measurement of decay times of 5 ps to 40 ns. The recorded traces were deconvoluted with the system response and fitted to an exponential function using the Fluofit (PicoQuant) windows program.

In femtosecond transient absorption measurements, Spectra-Physics Hurricane Titanium: Sapphire regenerative amplifier system was used as the laser system. The full spectrum setup was based on an optical parametric amplifier (Spectra-Physics OPA 800) as a pump. A residual fundamental light, from the pump OPA, was used for white light generation, which was detected with a CCD spectrograph. The OPA was used to generate excitation pulses at 480 nm. The laser output was typically $5 \mu\text{J pulse}^{-1}$ (130 fs fwhm) with a repetition rate of 1 kHz. The power dependence and the wavelength dependence were not studied. A circular cuvette ($d = 1.8$ cm, 1 mm, Hellma), with the sample solution, was placed in homemade rotating ball bearing (1000 rpm), to avoid local heating by the laser beam. The solutions of the samples were prepared to have an optical density at the excitation wavelength of ca. 0.5 in a 1 mm cell. The incremental time delay could be changed during the measurement. This allowed small steps at early times and larger steps at later times. All photophysical properties reported here have an error bar of 5–10%.

Acknowledgment. We thank the German Ministry for Education and Research (BMBF Netzwerk “Polymere Solarzellen”) for funding. J.C. thanks the “Fonds der Chemischen Industrie” and the German Ministry for Education and Research (BMBF) for a Kekulé Grant. A.P. thanks the EC, HPMT-CT-2001-00311. Financial support from NWO (Nederlandse Organisatie voor Wetenschappelijk Onderzoek) for the femtosecond equipment and from the UvA (Universiteit van Amsterdam) is gratefully acknowledged.

Supporting Information Available: Femtosecond transient absorption spectra of the reference compounds T₆ and PMI. This material is available free of charge via the Internet at <http://pubs.acs.org>.

References and Notes

- (1) Balzani, V., Ed. *Electron Transfer in Chemistry*; Wiley-VCH: New York, 2001; Vols. 1–5.
- (2) Wasielewski, M. R. *Chem. Rev.* **1992**, *92*, 435.
- (3) Paddon-Row, M. N. *Electron and Energy Transfer, in Stimulating Concepts in Chemistry*; Vögtle, F., Stoddart, J., Shibasaki, M., Eds.; Wiley-VCH: New York, 2000; pp 267–291.
- (4) O'Regan, B.; Grätzel, M. *Nature* **1991**, *353*, 737–739.
- (5) Ramos, A. M.; Meskers, S. C. J.; Van Hal, P. A.; Knol, J.; Hummel, J. C.; Janssen, R. A. J. *J. Phys. Chem. A* **2003**, *107*, 9269.
- (6) Bosman, A. W.; Janssen, H. M.; Meijer, E. W. *Chem. Rev.* **1999**, *99*, 1665.
- (7) Maus, M.; De, R.; Lor, M.; Weil, T.; Mitra, S.; Wiesler, U.-M.; Herrman, A.; Hofkens, J.; Vosch, T.; Mullen, K.; De Schryver, F. C. *J. Am. Chem. Soc.* **2001**, *123*, 7668.
- (8) Gronheid, R.; Hofkens, J.; Kohn, F.; Weil, T.; Reuther, E.; Mullen, K.; De Schryver, F. C. *J. Am. Chem. Soc.* **2002**, *124*, 2418.
- (9) Weil, T.; Wiesler, U. M.; Herrmann, A.; Bauer, R.; Hofkens, J.; De Schryver, F. C.; Mullen, K. *J. Am. Chem. Soc.* **2001**, *123*, 8101.
- (10) Maus, M.; Mitra, S.; Lor, M.; Hofkens, J.; Weil, T.; Herrman, A.; Mullen, K.; De Schryver, F. C. *J. Phys. Chem. A* **2001**, *105*, 3961.
- (11) Plavoets, M.; Vogtle, F.; De Cola, L.; Balzani, V. *New J. Chem.* **1999**, 63.
- (12) Dirksen, A.; De Cola, L. *C. R. Chim.* **2003**, *6*, 873.
- (13) Lor, M.; Thielemans, J.; Viaene, L.; Cotlet, M.; Hofkens, J.; Weil, T.; Hampel, C.; Mullen, K.; Verhoeven, J. W.; Van der Auweraer, M.; De Schryver, F. C. *J. Am. Chem. Soc.* **2002**, *124*, 9918.
- (14) Gosztoła, D.; Niemczyk, M. P.; Svec, W.; Lukas, A. S.; Wasielewski, M. R. *J. Phys. Chem. A* **2000**, *104*, 6545.
- (15) Wang, J. F.; Kawabe, Y.; Shaheen, S. E.; Morrel, M. M.; Jabbour, G. E.; Lee, P. A.; Anderson, J.; Armstrong, N. R.; Kippelen, B.; Mash, E. A.; Peyghambarian, N. *Adv. Mater.* **1998**, *10*, 230.
- (16) Borsenberger, P. M. *J. Appl. Phys.* **1990**, *68*, 5188.
- (17) Ikemoto, J.; Takimiya, K.; Aso, Y.; Otsubo, T.; Fujitsuka, M.; Ito, O. *Org. Lett.* **2002**, *4*, 309.
- (18) Hirayama, D.; Yamashiro, T.; Takimiya, K.; Aso, Y.; Otsubo, T.; Norieda, H.; Imahori, H.; Sakata, Y. *Chem. Lett.* **2000**, 570.
- (19) Fujitsuka, M.; Masuhara, A.; Kasai, H.; Oikawa, H.; Nakanishi, H.; Ito, O.; Yamashiro, T.; Aso, Y.; Otsubo, T. *J. Phys. Chem. B* **2001**, *105*, 9930.
- (20) Fujitsuka, M.; Ito, O.; Yamashiro, T.; Aso, Y.; Otsubo, T. *J. Phys. Chem. A* **2000**, *104*, 4876.
- (21) Gensch, T.; Hofkens, J.; Herrmann, A.; Tsuda, K.; Verheijen, W.; Vosch, T.; Christ, T.; Basché, T.; Müllen, K.; De Schryver, F. C. *Angew. Chem., Int. Ed. Engl.* **1999**, *38*, 3752.
- (22) Kirschbaum, T.; Briehn, C. A.; Bäuerle, P. *J. Chem. Soc., Perkin Trans. 1* **2000**, 1211.
- (23) Cremer, J.; Mena-Osteritz, E.; Pschirer, N.; Müllen, K.; Bäuerle, P. *Org. Biomol. Chem.* **2005**, *3*, 985–995.
- (24) Nicolas, N.; Fabre, B.; Simonet, J. *Electrochim.* **2001**, 3421.
- (25) Williams, R. M.; Zwier, J. M.; Verhoeven, J. W. *J. Am. Chem. Soc.* **1995**, *117*, 4093.
- (26) Jenneskens, L. W.; Verhey, H. J.; Vanramesdonk, H. J.; Verhoeven, J. W.; Vanmalssen, K. F.; Schenk, H. *Recl. Trav. Chim. Pays-Bas J. R. Neth. Chem. Soc.* **1992**, *111*, 507–510.
- (27) Oevering, H.; Paddon-Row, M. N.; Heppener, M.; Oliver, A. M.; Cotsaris, E.; Verhoeven, J. W.; Hush, N. S. *J. Am. Chem. Soc.* **1987**, *109*, 3258.
- (28) Eaton, D. E. *Pure Appl. Chem.* **1988**, *7*, 1107.
- (29) Ford, W. E.; Kamat, P. V. *J. Phys. Chem.* **1987**, *91*, 6373.
- (30) Tomizaki, K.; Loewe, R. S.; Kirmaier, C.; Schwartz, J. K.; Retsek, J. L.; Bocian, D. F.; Holten, D.; Lindsey, J. S. *J. Org. Chem.* **2002**, *67*, 6519.
- (31) Lap, D. P.; Grebner, D.; Rentsch, S. *J. Phys. Chem. A* **1997**, *101*, 107.
- (32) Wintgens, V.; Valat, P.; Garnier, F. *J. Phys. Chem.* **1994**, *98*, 228.
- (33) Emmi, S. S.; D'Angelantonio, M.; Beggiano, G.; Poggi, G.; Geri, A.; Pietropaolo, D.; Zotti, G. *Radiat. Phys. Chem.* **1999**, *54*, 263.
- (34) Sautter, A.; Kaletas, B. K.; Schmid, D. G.; Dobrawa, R.; Zimine, M.; Jung, G.; van Stokkum, I. H. M.; De Cola, L.; Williams, R. M.; Würthner, F. *J. Am. Chem. Soc.* **2005**, *127*, 6719.
- (35) Shida, T. *Electronic Absorption Spectra of Radical Ions (Physical Science Data; 34)*; Elsevier Science Publishers B. V.: New York, 1988.
- (36) Bonvoisin, J.; Launay, J.-P.; Van der Auweraer, M.; De Schryver, F. C. *J. Phys. Chem.* **1994**, *98*, 5052.
- (37) Kaletas, B. K.; Dobrawa, R.; Sautter, A.; Würthner, F.; Zimine, M.; De Cola, L.; Williams, R. M. *J. Phys. Chem. A* **2004**, *108*, 1900.
- (38) Weller, A. *Z. f. Phys. Chem., Neue Folge.* **1982**, *133*, 93.
- (39) Oyama, M.; Kambayashi, M. *Electrochem. Commun.* **2002**, *4*, 759.
- (40) Frere, P.; Raimundo, J. M.; Blanchard, P.; Delaunay, J.; Richomme, P.; Sauvajol, J. L.; Orduna, J.; Garin, J.; Roncali, J. *J. Org. Chem.* **2003**, *68*, 7254.
- (41) Marcus, R. A.; Sutin, N. *Biochim. Biophys. Acta* **1985**, *811*, 265.
- (42) Fron, E.; Lor, M.; Pilot, R.; Schweitzer, G.; Dincalp, H.; De Feyter, S.; Cremer, J.; Bäuerle, P.; Mullen, K.; Van der Auweraer, M.; De Schryver, F. C. *Photochem. Photobiol. Sci.* **2005**, *4*, 61–68.